Appl. Phys. B 87, 717–722 (2007)
DOI: 10.1007/s00340-007-2637-3

Applied Physics B
Lasers and Optics

Y. QIAO[1,2]
N. DA[1]
D. CHEN[1,✉]
Q. ZHOU[1]
J. QIU[1,3]
T. AKAI[4]

Spectroscopic properties of neodymium doped high silica glass and aluminum codoping effects on the enhancement of fluorescence emission

[1] Photo Craft Project, Shanghai Institute of Optics and Fine Mechanics, Chinese Academy of Sciences, 201800 Shanghai, P.R. China
[2] Graduate School of the Chinese Academy of Sciences, 100080 Beijing, P.R. China
[3] College of Materials Science and Chemical Engineering, Zhejiang University, 310027 Hangzhou, P.R. China
[4] National Institute of Advanced Industrial Science and Technology Osaka, 563-8577 Osaka, Japan

Received: 5 November 2006 / Revised version: 22 January 2007
Published online: 17 May 2007 • © Springer-Verlag 2007

ABSTRACT Nd^{3+}-codoped and Al^{3+}-Nd^{3+}-codoped high silica glasses have been prepared by sintering nanoporous glasses impregnated with Nd^{3+} and Al^{3+} ions. The Judd–Ofelt intensity parameters $\Omega_{2,4,6}$ of Nd^{3+}-doped high silica glasses were obtained and used to analyze aluminum codoping effects. Fluorescence properties of Nd^{3+}-doped high silica glasses strongly depend on the Al^{3+} concentration. While Nd^{3+} ion absorption and emission intensities of obviously increase when aluminum is added to Nd^{3+}-doped high silica glasses, fluorescence lifetimes decrease and aluminum codoping has almost no influence on the radiative quantum efficiencies. This indicates that aluminum codoping is responsible for an anti-quenching effect through a local modification of rare-earth environments rather than through physical cluster dispersion.

PACS 78.55.Qr; 42.70.-a

1 Introduction

Silica glass is an attractive host matrix for the rare-earth ions because of its fine optical and mechanical properties, such as good chemical stability, high UV transparency, strong thermal resistance, low nonlinear index or refractive, high surface damage threshold to lasers and large tensile fracture strength. Concentration quenching, however, limits the application of rare-earth-doped silica laser glass used as a host matrix. For example, in the silica glasses melted by conventional methods, Nd^{3+} clustering becomes prominent when the neodymium concentration exceeds 0.5 wt. % [1]. Concentration quenching is related to the energy levels and transitions of active ions, as well as the distances between them in materials, thereby involving the active ions' environment [2]. Various methods have been attempted to avoid clustering of rare-earth ions and concentration quenching in silica glasses, including plasma-torch chemical vapor deposition (CVD) [3], sol–gel [4] and modified sol–gel methods using zeolite X [5]. Recently, several groups have adopted a new method to disperse RE (rare-earth) ions in SiO_2 glass. They have fabricated rare-earth-doped high silica glasses based on porous silica glass techniques [6, 7]. Good performance from Nd^{3+}-doped high silica glass microchip lasers operating at 1.064 μm have been successfully demonstrated, suggesting that high silica glasses have potential for use as host materials for high-power and high-frequency solid-state lasers [8].

The effect of aluminum codoping on the fluorescence and structural properties of rare-earth-doped silica glasses has been previously reported, with most studies based on the plama-torch chemical vapor deposition method [3], sol–gel method [9] and other traditional glass melting methods. It is generally held [3] that RE ions are easily partitioned by Al^{3+}, forming Al–O–RE bonds rather than clustering and forming RE–O–RE bonds. This results in larger spacing among RE ions in the alumina-doped silica host compared to the non-alumina-containing host. Monteil et al., however, have recently analyzed the effect of aluminum on rare-earth clustering in glasses by molecular dynamics simulation [10]. Simulation results show that rare-earth ions are preferentially located in aluminum-rich domains, while the local structure around rare-earth ions is affected by aluminum through a structuring effect. This aluminum effect is responsible for differences in structure of the luminescent sites rather than in an effective dispersion of the rare-earth ions. Investigation of the effect of aluminum ions on the Nd^{3+}-codoped high silica glass may provide an experimental method to test these results. In the present work, the sintering nanoporous glass method was used to fabricate Al^{3+}-Nd^{3+}-codoped high silica glasses and Judd–Ofelt intensity parameters $\Omega_{2,4,6}$ were used to discuss the effect of aluminum codoping on the structure and fluorescence properties of Nd^{3+}-doped high silica glass.

2 Experimental

Porous silica glass was obtained by removing the borate phase from phase-separated alkali-borosilicate glass by repeatedly washing and leaching with hot acid solutions [11]. The analytical composition of the porous glass

✉ Fax: +86-21-59929373, E-mail: dpchen2008@yahoo.com.cn

obtained by phase separating and acid treating was 97.0% $SiO_2 \cdot 2.1\%\ B_2O_3 \cdot 0.8\%\ Al_2O_3 \cdot 0.1\%$ ($Na_2O + CaO$). Porous glass is a transparent material whose pore sizes are less than 40 Å, with pores nominally occupying about 40% of the glass volume. The porous glasses were immersed in solutions of $Nd(NO_3)_3 \cdot 6H_2O$ or mixed solutions of $Nd(NO_3)_3 \cdot 6H_2O$ and $Al(NO_3)_3 \cdot 9H_2O$ for $0.5 \sim 1.0$ h and dried at room temperature. The porous glasses impregnated with active ions were then sintered at 1100 °C for 2 h to obtain the final samples. Two series of high silica glass samples were produced for comparison:

1. Nd^{3+}-doped high silica glasses: the concentration of $Nd(NO_3)_3$ solution varied from 0.05 to 0.75 mol/L;
2. Al^{3+}-Nd^{3+}-codoped high silica glasses: the Al/Nd mole ratio was varied from 1 to 15. Higher Al/Nd mole ratio high silica glass was not prepared because of the solubility limit of $Al(NO_3)_3$ in distilled water. The final samples obtained all looked compact, azury and transparent. The glass samples were cut and polished to $10 \times 10 \times 1.5$ mm for the next measurements. There was no visible difference between the Nd^{3+}-doped and Al^{3+}-Nd^{3+}-codoped samples.

Sample density was measured using the buoyancy method based on Archimedes principle using distilled water as the immersion liquid. The refractive index was measured with an Abbe refractometer. The density was 1.98 g/cm^3 and the refraction index 1.462. The absorption spectra were recorded with a Jasco V-570 UV/VIS/NIR spectrophotometer. The infrared luminescent spectra were obtained with ZOLIX SBP300 spectrophotometer under 808nm LD excitation. The fluorescence lifetime was recorded with a modulated 808 nm LD with a maximum power of 2 W The frequency was modulated at 100 Hz and the signal, detected by an InGaAs photodetector in TRIAX550, was recorded using a storage digital oscilloscope (Tektronix TDS3052). Errors in the absorption, fluorescence, and lifetime measurements were estimated to be under ±5%, ±10%, and ±10%, respectively. All measurements were made at room temperature.

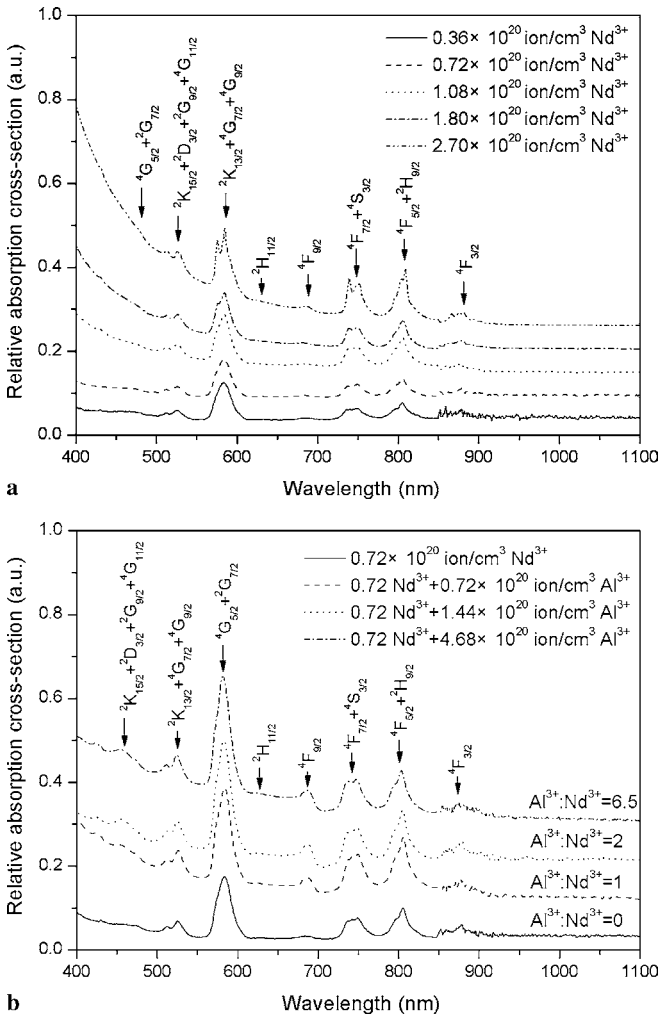

FIGURE 1 Absorption spectra of (**a**) Nd^{3+}-doped high silica glasses with different Nd^{3+} concentration, (**b**) Al^{3+}-Nd^{3+}-codoped high silica glasses with different Al/Nd mole ratio

3 Results and discussion

The relative absorption cross-section of Nd^{3+}-doped high silica glasses with different Nd^{3+} concentrations and Al^{3+}-Nd^{3+}-codoped high silica glasses with different Al/Nd mole ratios are shown in Fig. 1a and b. Adding aluminum ions increases the absorption cross-section of Nd^{3+}-doped high silica glasses as shown in Fig. 1b. For Nd^{3+}, the electric-dipole transitions are predominant. The line strengths of the electric-dipole transitions from the ground $^4I_{9/2}$ manifold to the excited J'-manifold can be obtained by the following relation [12]

$$S_{\mathrm{mea}}(J \to J') = \frac{3hc(2J+1)}{8\pi^3 e^2 \lambda_{\mathrm{p}}} \frac{9n}{(n^2+2)^2 N_0} \int \kappa(\lambda)\,\mathrm{d}\lambda\,, \qquad (1)$$

where N_0 is the Nd^{3+} concentration expressed in ion/cm^3, n is the refractive index of the sample, λ_{p} is the peak wavelength of the absorption band and κ is the absorption coefficient at wavelength λ. According to the Judd–Ofelt theory [13, 14], the line strength can also be expressed as

$$S_{\mathrm{cal}}(J \to J') = \sum_{t=2,4,6} \Omega_t \left|\left\langle 4f^n\,[\alpha SL]\,J \left\| U^{(t)} \right\| 4f^n\left[\alpha' S' L'\right] J' \right\rangle\right|^2\,, \qquad (2)$$

where the elements $U^{(t)}$ ($t = 2, 4, 6$) are the doubly reduced unit tensor operators calculated in the intermediate coupling approximation, which is almost independent of a change of host [15]. Intensity parameters Ω_t ($t = 2, 4, 6$) are phenomenologically independent of electronic quantum numbers with the ground $4f^3$ configuration of a Nd^{3+} ion. By a least-root-mean-square (rms) fitting between (1) and (3), the three intensity parameters $\Omega_{2,4,6}$ could be obtained. The intensity parameters $\Omega_{2,4,6}$ of Al^{3+}-Nd^{3+}-codoped high silica glasses with different composition are listed in Table 1. Because of the inhomogeneous broadening, some excited levels of Nd^{3+} are generally not resolved. In this study, six absorption bands that correspond to the transitions from the ground state $^4I_{9/2}$ level to the excited levels $^4F_{3/2}$, $^4F_{5/2} + {}^2H_{9/2}$, $^4F_{7/2} + {}^4S_{3/2}$, $^4F_{9/2}$, $^4G_{5/2} + {}^2G_{7/2}$, and $^2K_{13/2} + {}^4G_{7/2} + {}^4G_{9/2}$ are used for fitting.

sample	Al^{3+} (10^{20} ion/cm^3)	Nd^{3+} (10^{20} ion/cm^3)	Al/Nd mole ratio	$\Omega_{2,4,6}$ (10^{-20} cm^2) Ω_2	Ω_4	Ω_6
1	0	0.36	0	5.07	3.98	2.24
2	0	1.43	0	5.34	3.20	4.31
3	0	1.79	0	5.64	3.22	4.48
4	1.80	0.36	5	7.16	3.20	2.97
5	0.72	0.72	1	8.20	4.95	4.59
6	3.22	1.07	3	8.85	4.48	4.10

TABLE 1 Intensity parameters $\Omega_{2,4,6}$ of Al^{3+}-Nd^{3+}-codoped high silica glasses with different Al/Nd mole ratio

For silica glasses made by conventional methods, the clustering of Nd^{3+} ions occur at concentrations of several hundred ppm [16] and the absorption intensity of Nd^{3+}-doped silica glass is too low to analyze spectroscopic properties using Judd–Ofelt calculations. In high silica glasses, however, the nanoporous structure helps to disperse the Nd^{3+} ions uniformly and evidently improves the solubility of Nd^{3+} ions [8]. Several reasons for the improvement of the Nd^{3+}-doped concentration in high silica glasses have been inferred. The first is due to the nanopore effect. After repeated hot acid solution leaching and washing, nanoporous glasses have large specific surface areas and high surface activity. When nanoporous glasses are immersed in $Nd(NO_3)_3 \cdot 6H_2O$ solutions, Nd^{3+} ions firmly cling to the surface of the pores, reducing surface activity. In this way Nd^{3+} ions are dispersed uniformly on the large specific surface of the nanoporous glasses. Another reason for the improvement is the existence of dangling bonds. The repeated hot acid processing of nanoporous glass leaves large numbers of dangling bonds on the surface of the pores, such as various Si–O– bonds from SiO_4 units losing one or two oxygens, as well as O–Si–, B–O– and Al–O– bonds. These active dangling bonds strongly attract Nd^{3+} cations to form various stable Si–O–Nd and B–O–Nd bonds. An additional reason is the sintering temperature of high silica glasses. At only 1100°, it is not enough to melt porous silica glass. The Nd^{3+} ions in solid state glasses move with difficulty during the sintering process and clustering becomes more difficult in high silica glasses.

Among the three intensity parameters, the Ω_2 parameter reflects the intensity of the hypersensitive transition, whereas the Ω_4 and the Ω_6 parameters give an indication of the overall intensity of the spectral transition. Ω_2 is most sensitive to local structure and glass composition, which reflects the amount of covalent bonding and the asymmetry of the local environment near the rare-earth site. As seen in Table 1, two points are of particular interest. First, the Ω_2 value of Nd^{3+}-doped high silica glass is over 5.0×10^{-20} cm^2, larger than most of values of silicate [17], fluoride [18], phosphate [19], borate [20] and aluminate [21]. The large Ω_2 value suggests a lower centrosymmetric coordination environment around the Nd^{3+} in high silica glass. As mentioned above, there are various dangling bonds with high activity in nanoporous glass and they can strongly attract Nd^{3+} cations to form various Si–O–Nd and B–O–Nd bonds. These confused environments induce low symmetry around Nd^{3+} ions in Nd^{3+}-doped high silica glasses. Additionally, the values of Ω_2 become higher when the concentration of Al^{3+} ions increase, indicating that the asymmetry of the local environment near Nd^{3+} sites becomes lower. Aluminum randomly distributes around Nd^{3+} ions and creates a relatively low symmetry environment around the neodymium ions.

Figure 2 shows the fluorescence spectrum of Nd^{3+}-doped (Nd^{3+} concentration: 0.36×10^{20} ion/cm^3) high silica glass without aluminum codoping. The inset shows the intensities of the $^4F_{3/2} \rightarrow {}^4I_{11/2}$ transitions as a function of Nd^{3+} concentration. The fluorescence intensity gets to the maximum when the Nd^{3+} concentration is 0.72×10^{20} ion/cm^3.

Figure 3 shows fluorescence spectra of Nd^{3+}-doped and Al^{3+}-Nd^{3+}-codoped (Al/Nd = 5) high silica glasses. We can observe an obvious enhancement in fluorescence intensity after aluminum ions were codoped into the high silica glass, as shown in Fig. 3a. The fluorescence intensity of Al^{3+}-Nd^{3+}-codoped (Al/Nd = 5) high silica glass is about 3.5 times higher than that of the Nd^{3+}-doped high silica glass. The fluorescence spectra of Nd^{3+}-doped high silica glasses with various aluminum concentrations are shown in Fig. 3b. No significant peak wavelength shift or line-shape change was observed when the Al/Nd mole ratio was changed within the sampled range, indicating that these parameters depend weakly on the Al/Nd mole ratio. The fluorescence intensity, however, strongly depends on the Al^{3+} concentration, with the strongest emission occuring at Al/Nd = 8. This value is very close to the concentration necessary for a cluster-free Nd^{3+}-doped silica glass made by CVD, as determined by Arai et al [3]. The strong enhancement of fluorescence after codoping aluminum clearly demonstrates that aluminum ions change the local environment around Nd^{3+} ions. Codoped aluminum is available to accommodate the Nd^{3+} ions in a more energetically favorable environment.

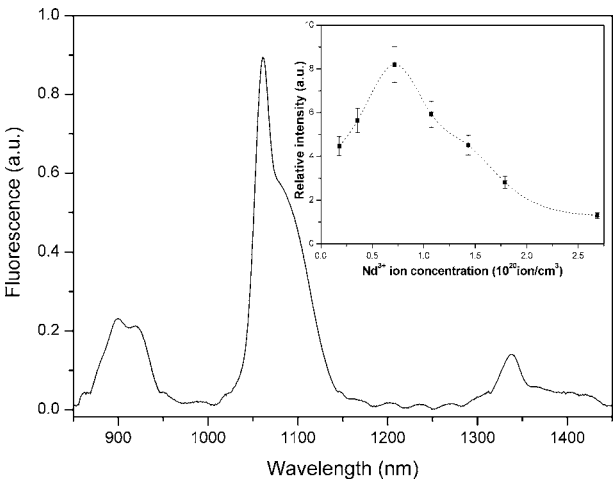

FIGURE 2 Fluorescence spectrum of Nd^{3+}-doped (Nd^{3+} concentration: 0.36×10^{20} ion/cm^3) high silica glass. The *inset* shows the intensities of the $^4F_{3/2} \rightarrow {}^4I_{11/2}$ transitions as a function of Nd^{3+} concentration

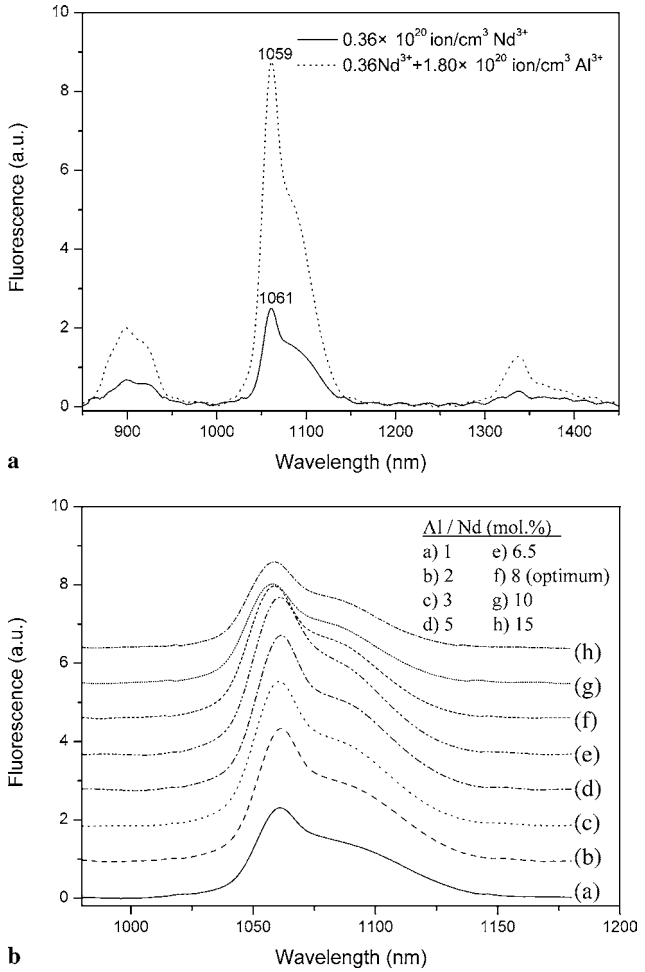

FIGURE 3 Fluorescence spectra of (**a**) Nd^{3+}-doped and Al^{3+}-Nd^{3+}-codoped high silica glasses, (**b**) the ${}^4F_{3/2} \rightarrow {}^4I_{11/2}$ transitions of Nd^{3+} in Al^{3+}-Nd^{3+}-codoped high silica glasses with various Al/Nd mole ratios

The fluorescence lifetimes of Nd^{3+}-doped high silica glasses as a function of Nd^{3+} concentration are shown in Fig. 4. The fluorescence lifetimes decrease with increasing Nd_2O_3 concentration. It decreases from 360 μs at 0.18×10^{20} ion/cm^3 to 290 μs at 2.7×10^{20} ion/cm^3 Nd^{3+}. Fluorescence lifetimes of Al^{3+}-Nd^{3+}-doped high silica glasses were also measured. The lifetimes shorten after adding aluminum ions to the high silica glasses. The lifetimes are 250 μs and 240 μs when the mole ratios are Al/Nd = 2 and Al/Nd = 6.5, respectively. The transfer process of Nd^{3+} ions from excited energy levels to the ground energy level becomes faster in Al^{3+}-Nd^{3+}-codoped high silica glasses.

Spontaneous emission probabilities $A^{\mathrm{ed}}_{JJ'}$, corresponding to transitions from the ${}^4F_{3/2}$ manifold, which are generally used as the upper level for the Nd^{3+}-doped solid-state laser, to the lower J'-manifolds ${}^4I_{J'}$ can be calculated by means of the following relation [12]

$$A^{\mathrm{ed}}_{JJ'}(J \rightarrow J') = \frac{64\pi^4 e^2}{3h(2J+1)\lambda_{\mathrm{e}}^3} \frac{n(n^2+2)^2}{9} \times \sum_{t=2,4,6} \Omega_t \left| \left\langle {}^4F_{3/2} \left\| U^{(t)} \right\| {}^4I_{J'} \right\rangle \right|^2 , \quad (3)$$

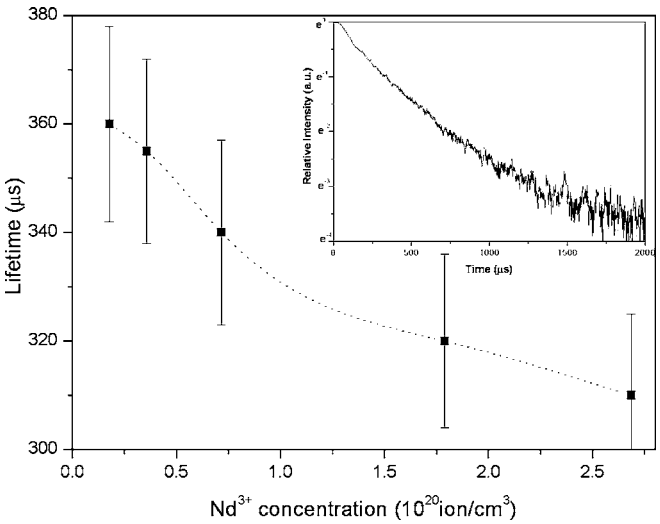

FIGURE 4 Fluorescence lifetimes of Nd^{3+}-doped high silica glasses as a function of Nd^{3+} concentration. The inset shows the decay curve of Nd^{3+}-doped (Nd^{3+} concentration: 0.72×10^{20} ion/cm^3) high silica glass

where λ_{e} is the peak wavelength of emission bands and the values of $U^{(t)}$ ($t = 2, 4, 6$) have been proposed by Kaminskii et al. [22]. The fluorescence lifetime of the ${}^4F_{3/2}$ manifold is

$$\tau_{\mathrm{c}} = \frac{1}{\sum_{J'} A^{\mathrm{ed}}_{JJ'}} , \quad (4)$$

The Nd^{3+} fluorescence bands are asymmetric, therefore an effective linewidth $\Delta\lambda_{\mathrm{eff}}$ is defined by [23]

$$\Delta\lambda_{\mathrm{eff}} = \frac{\int I(\lambda)\,\mathrm{d}\lambda}{I_{\max}} , \quad (5)$$

where $I(\lambda)$ is the emission intensity at wavelength λ and $I_{\max}$ is the emission intensity at peak emission wavelength. The stimulated emission cross-sections of the transition ${}^4F_{3/2} \rightarrow {}^4I_{11/2}$ at 1060 nm was estimated from the fluorescence spectra by [23]

$$\sigma_{1.06} = \frac{\lambda_{\mathrm{e}}^4}{8\pi c n^2 \Delta\lambda_{\mathrm{eff}}} A\left({}^4F_{3/2} \rightarrow {}^4I_{11/2}\right) , \quad (6)$$

where spontaneous emission probability $A({}^4F_{3/2} \rightarrow {}^4I_{11/2})$ is obtained by (4). Table 2 lists the values of λ_{e}, $\Delta\lambda_{\mathrm{eff}}$, $\sigma_{1.06}$, τ_{c}, τ_{m} and η of some Al^{3+}-Nd^{3+}-codoped high silica glasses. τ_{c} is the fluorescence lifetime calculated by (5) and τ_{m} is the fluorescence lifetime obtained from the fluorescence decay curve. The radiative quantum efficiency is defined as

$$\eta = \frac{\tau_{\mathrm{m}}}{\tau_{\mathrm{c}}} . \quad (7)$$

In laser glasses, a large stimulated emission cross-section is beneficial for a low threshold and a high gain in laser operations. As shown in Table 2, Al^{3+}-Nd^{3+}-codoped high silica glasses have stimulated emission cross-sections that are larger than those of Nd^{3+}-doped high silica glasses. This shows that adding aluminum to high silica glasses helps improve its stimulated emission cross-section. We have also noticed that despite decreases in the fluorescence lifetime when aluminum

TABLE 2 Values of λ_e, $\Delta\lambda_{eff}$, $\sigma_{1.06}$, τ_c, τ_m and η of some Al^{3+}-Nd^{3+}-codoped high silica glasses

Glass sample	Al^{3+} (10^{20} ion/cm^3)	Al/Nd (mole ratio)	λ_e (nm)	$\Delta\lambda_{eff}$ (nm)	$\sigma_{1.06}$ (10^{-20} cm^2)	τ_c (μs)	τ_m (μs)	η (%)
a	0.72	0	1061	48.41	2.23	748	355	47.5
b	0.72	2	1061	46.83	3.31	538	250	46.5
c	0.72	6.5	1061	44.98	3.44	507	240	47.3

is codoped into high silica glasses, the radiative quantum efficiencies between Nd^{3+}-doped and Al^{3+}-Nd^{3+}-codoped high silica glasses show no remarkable differences. Aluminum codoping seemingly has almost has no influence on the radiative quantum efficiency of Nd^{3+} ions.

It is commonly held that the aluminum effect promotes cluster dispersion and that concentration quenching is restrained through the physical cluster dispersion of aluminum [3]. In this study, however, there is no clear evidence to prove the existence of a dispersion effect due to aluminum. If aluminum was not clustered but instead partitioned rare-earth ions to form Al-O-Nd, cross relaxation between Nd^{3+} ions would be restrained in aluminum codoped high silica glass matrices and the radiative quantum efficiency would correspondingly increase.

In this study, absorption and fluorescence intensities were remarkably enhanced when aluminum was added to high silica glasses, but fluorescence lifetimes decreased and radiative quantum efficiencies did not significantly change. The modification of structures around Nd^{3+} ions is thought to be the primary cause of changes in spectroscopic properties. According to the model and simulations of Monteil et al. [10], aluminum is always located near RE ions and the aluminum effect on the RE ions occurs mainly through a local modification of the RE environments. In the snapshot [10] of the aluminum codoped simulated structure, the clusters are clearly identifiable and aluminum codoping does not seem to prevent clustering. The modification of aluminum around RE ions appears to be a reorganization of atoms owing to more defined distances and angles. The authors explain that these so-called new sites correspond to high energy sites and they have consequences for Al-RE-codoped glass spectroscopy. Alombert-Goget et al. [24] recently studied the spectroscopic properties of Eu_2O_3-Al_2O_3-SiO_2 glasses codoped with aluminum. They explain the Eu^{3+} spectroscopic results by assuming that "the incorporation of Al^{3+} in silica increases the network flexibility and modifies the crystal field strength around the Eu^{3+} ion as well as the axial distortion".

Our experimental results seem to agree with the model of Monteil et al. Aluminum codoping obviously decreased fluorescence lifetimes and did not improve radiative quantum efficiencies. There was no clear dispersion effect in Al^{3+}-Nd^{3+}-codoped high silica glasses. The local structure around Nd^{3+} ions was reorganized by aluminum codoping and the reorganization caused the diversity of luminescent sites for Nd^{3+} ions.

4 Conclusion

A method was developed to produce Nd^{3+}-doped and Al^{3+}-Nd^{3+}-codoped high silica glasses by sintering nanoporous glass. Following the Judd–Ofelt theory, the three intensity parameters $\Omega_{2,4,6}$ were obtained from the absorption spectra of Nd^{3+}-doped high silica glasses. The large Ω_2 values suggest a low centrosymmetric coordination environment around the Nd^{3+} in high silica glasses. In these glasses, nanoporous structures can disperse the Nd^{3+} ions uniformly and evidently improve the solubility of Nd^{3+} ions. The fluorescence intensity reaches a maximum when the Nd^{3+} concentration is 0.72×10^{20} ion/cm^3 in Nd^{3+}-doped high silica glasses.

The fluorescence intensity was observed to vary significantly with changes in aluminum concentration and the strongest emission was obtained with an Al/Nd mole ratio of 8, indicating a strong dependence of the fluorescence intensity on the Al^{3+} concentration. Comparison of the spectroscopic properties of Nd^{3+}-doped and Al^{3+}-Nd^{3+}-codoped high silica glasses show that absorption and fluorescence intensities are remarkably enhanced when aluminum is added to high silica glasses, but fluorescence lifetimes decrease and radiative quantum efficiency do not significantly change. There is no clear evidence to prove the dispersion effect of aluminum and cross relaxation has not been effectively restrained in codoped glasses in this study. Our study indicates that the remarkable increase in fluorescence intensity is responsible for the aluminum codoping effect through a local modification of the RE environments rather than through physical cluster dispersion. We also show that Al^{3+}-Nd^{3+}-codoped high silica glasses have larger stimulated emission cross-sections than that of Nd^{3+}-doped high silica glasses. RE-doped high silica glasses obtained by methods used for porous glass are likely to be new materials used for high power and high repetition rate lasers.

ACKNOWLEDGEMENTS We would like to acknowledge financial support from the National Natural Science Foundation of China (Grant No. 50125258 and 60377040).

REFERENCES

1 E.I. Galant, Y.N. Kondrat'ev, A.K. Przhevuskii, T.I. Prokhorova, M.N. Tolstoi, V.N. Shapovalov, JETP Lett. **18**, 373 (1973)
2 J.A. Caird, A.J. Ramponi, P.R. Staver, J. Opt. Soc. Am. B **7**, 1391 (1991)
3 K. Arai, H. Namikawa, K. Kumata, T. Honda, Y. Ishii, T. Handa, J. Appl. Phys. **59**, 3430 (1986)
4 I.M. Thomas, S.A. Payne, G.D. Wilke, J. Non-Cryst. Solids **151**, 183 (1992)
5 Y. Fujimoto, M. Nakatsuka, J. Non-Cryst. Solids **215**, 182 (1997)
6 D. Chen, H. Miyoshi, T. Akai, T. Tazawa, Appl. Phys. Lett. **86**, 231 908 (2005)
7 W. Liu, D. Chen, H. Miyoshi, K. Kadono, T. Akai, Chem. Lett. **34**, 1176 (2005)
8 J. Xia, D. Chen, J. Qiu, C. Zhu, Opt. Lett. **30**, 47 (2005)
9 Y. Zhou, Y.L. Lam, S.S. Wang, H.L. Liu, C.H. Kam, Y.C. Chan, Appl. Phys. Lett. **71**, 587 (1997)
10 A. Monteil, S. Chaussedent, G. Alombert-Goget, N. Gaumer, J. Obriot, S.J.L. Ribeiro, Y. Messaddeq, A. Chiasera, M. Ferrai, J. Non-Cryst. Solids **348**, 44 (2004)
11 W. Liu, D. Chen, H. Miyoshi, K. Kadono, T. Akai, J. Non-Cryst. Solids **352**, 2969 (2006)
12 W.F. Krupke, Phys. Rev. **145**, 325 (1966)
13 B.R. Judd, Phys. Rev. **127**, 750 (1962)

14 G.S. Ofelt, J. Chem. Phys. **37**, 511 (1962)
15 W.T. Carnall, P.R. Fields, K. Rajnak, J. Chem. Phys. **49**, 4424 (1968)
16 S. Sen, J.F. Stebbins, J. Non-Cryst. Solids **188**, 54 (1995)
17 R.R. Jacobs, M.J. Weber, IEEE J. Quantum Electron. **QE-10**, 450 (1974)
18 R. Balda, J. Fernández, A. Mendioroz, J.L. Adam, B. Boulard, J. Phys.: Condens. Matter **6**, 913 (1994)
19 Y. Nageno, H. Takabe, K. Morinaga, J. Am. Ceram. Soc. **76**, 3081 (1993)
20 K. Gatterer, G. Pucker, H.P. Fritzer, S. Arafa, J. Non-Cryst. Solids **176**, 237 (1994)
21 E.V. Uhlmann, M.C. Weinberg, N.J. Kreidl, L.L. Burgner, R. Zanoni, K.H. Church, J. Non-Cryst. Solids **178**, 15 (1994)
22 A.A. Kaminskii, G. Boulon, M. Buocristiani, B.D. Bartolo, A. Kornienko, V. Mironov, Phys. Stat. Solidi A **141**, 471 (1994)
23 M.J. Weber, J.D. Myers, D.H. Blackburn, J. Appl. Phys. **52**, 2944 (1981)
24 G. Alombert-Goget, N. Gaumer, J. Obriot, A. Rammal, S. Chaussedent, A. Monteil, H. Portales, A. Chiasera, M. Ferrari, J. Non-Cryst. Solids **351**, 1754 (2005)